Research article

Synthesis, characterization, DFT studies and evaluation of the potential anti-tumour activity of nicotinic hydrazide based Schiff base using in vitro and molecular docking techniques

V. Preethi, V.G. Vijukumar, S. AnilaRaj, V.G. Vidya [*]

Department of Chemistry, University College, Paalayam, Thiruvananthapuram, 695034, Kerala, India

ABSTRACT

Breast cancer, one of the most serious issues worldwide, has been raising day by day. It has now become a necessary to develop a suitable drug to combat this terrible illness. Schiff bases are increasingly being used as powerful medications for a number of illnesses. BNH has now synthesized from Benzil and Nicotinic hydrazide and characterized experimentally by FT-IR, UV, ^{1}H NMR, ^{13}CNMR and Mass analysis. DFT calculations were done using Gaussian 16 W with B3LYP/6-311 + G (d,p) and geometry of the compound is optimized. Frontier Molecular orbit (FMO), Mullikan atomic charges and Molecular Electrostatic Potential (MEP) were studied. Invitro antimicrobial studies were done using various bacteria and fungi. The synthesized compound is appropriate against bacterial and fungal actions. Invitro study were done using MCF-7 cell lines to analyze the anticancer property of the ligand. The outcome suggests that BNH may be employed in the future as a novel anticancer medication.

1. Introduction

Cancer is a disease that is becoming a threat to the people of the world. It is something deleterious enough to devour mankind. More than 19.3 million cancer cases and proximately 10 million cancer death cases were reported recently [1]. The fact is that it has not yet been possible to find a felicitous remedy for this disease that kills human life. It has become imperative to get hold of this deadly disease which is increasing day by day. There is an uncontrollable cell magnification which can affect different organs of the body and exhibits sundry symptoms [2]. To prevent this, we have to resort to coerced treatment methods and medicines. Cancer reporting has increased steadily over the past several years, and breast cancer is one of the most prevalent types. According to the current statistics, more cases were reported in developed countries than developing countries. Women are disproportionately affected and the remaining cases are visually perceived primarily by men. This rate appears to be increasing [3]. Various reasons increase the risk of this disease. Studies show that late pregnancy, menopause, lifestyle, incongruous diet, age, gender and utilization of variant of contraceptives all contribute to this disease [3,4]. Family tradition additionally contribute to this to some extent. There is growing need to develop a suitable treatment modality to surmount this life-threatening condition. Therefore, scientists are doing a lot of research to find surmount drugs for this. Schiff bases and its complexes can contribute a lot in the pharmaceutical area to fight against breast cancer.

Primary amines and carbonyl compounds condense to form Schiff bases [5]. The imino group, which is present in the Schiff base, forms hydrogen bonds with the active site of the reaction center and triggers a variety of reactions. The usage of Schiff base complexes

as a catalyst in numerous processes, including oxygenation, decomposition, hydrolysis etc. [6]. Living organisms were at risk from bacterial and fungal infections. Moreover, there is the growing problem of antimicrobial drug resistance, which negatively affects the health of living organisms because many infectious diseases are no longer effectively treated with over-the-counter drugs, resulting in a significant number of deaths worldwide. Schiff bases shows antibacterial and antifungal properties [7]. It also shows antituberculosis, antimalarial, anti-inflammatory applications etc. [8,9]. Many cancers, including those of the breast, lungs, glioblastoma, numerous neurological illnesses, etc., have been found to respond well to treatments including Schiff bases [10,11]. Hence, the contributions given by Schiff bases in medicinal and pharmaceutical fields is of great paramountcy Because of these multiple uses, interest in research on Schiff bases is growing, which inspires scientists to create novel compounds and make them useful in the treatment of major health problems.

Also, theoretical ways for creating suitable medications are emerging these days. Among them, computational chemistry appears to be increasingly prevalent. The electrical structure of molecules and solids can be studied using two well-known computational chemistry techniques: ab initio calculations [12] and Density Functional Theory (DFT). Both methods are essential for deciphering experimental data, forecasting molecular activity, and comprehending chemical characteristics. Density functional theory (DFT) has risen to prominence in theoretical molecular modelling rapidly. Comparing the DFT approach against traditional ab initio methods, the former can compute a wide range of molecular properties more precisely. Literature reviews showed that DFT is significantly more accurate at reproducing the geometrical structural values that are shown in experiments [13,14].

In the present study, a Schiff base (N′, N‴Z)-N′, N‴-(1,2-diphenylethane-1,2-diylidene) di (nicotinohydrazide) BNH is synthesized by the reaction between Benzil and Nicotinic hydrazide. The ligand was characterized experimentally using FT-IR, UV, ^{1}H and ^{13}C NMR as well as mass spectrometry and other instrumental methods. The DFT approach was used for theoretical computations, and the optimized geometry was produced. Various noncovalent interactions including hydrogen bond van be calculated using DFT [15]. The precise molecular geometries, activation energies, and energy differences between pairs of tautomer have been obtained using the widely used B3LYP approach. The B3LYP approach has been shown to be a good fit for systems due to its small absolute mistakes and cost-effectiveness of computations [16]. Thermochemical parameters of the ligand, its HOMO-LUMO transitions, MEP plot and Mulliken charge distribution was also obtained. *In vitro* experiments were used to evaluate the synthetic compound's biological properties. Gram-positive and Gram-negative bacteria were used to study the antibacterial and two fungi, which were chosen for antifungal properties. In order to determine the efficiency of the synthesized compound against breast cancer treatments, an *invitro* anticancer investigation was performed using MCF-7 breast cancer cells. Also docking technique, molecular docking was performed to analyze the interaction between synthesized ligand and various selected protein.

2. Materials and methods

Materials used for the synthesis of the ligand was of analytical grade and used without any purification. Benzil, Nicotinic hydrazide were purchased from Sigma Aldrich and used without any purification. FTIR of the synthesized ligand was obtained using PerkinElmer IR Version 10.6.0 in the region of 4000 cm^{-1} – 400 cm^{-1}. UV of the ligand was recorded using UV-2600 series spectrometer in the range of 200–600 nm using ethanol as solvent. ^{1}H NMR and ^{13}C NMR was recorded using Bruker Advance 400 MHz FT-NMR Spectrometer using DMSO as solvent. Molecular docking was performed using CB dock tool. DFT calculations were done using Gaussian 16 W software and visualised using Gauss View 6.1 software. Invitro anticancer studies were done using MCF cell lines collected from National Centre for Cell Sciences (NCCS), Pune, India.

3. ExperimentalPreparation of (N',N‴Z)-N′, N‴-(1,2-diphenylethane-1,2-diylidene)di (nicotinohydrazide) (BNH)

BNH was synthesized in accordance with the procedure described in Ref. [17]. A solution containing equal molar amounts of Benzil (2.1 g, 10 mmol) and Nicotinic hydrazide (1.37 g, 10 mmol) was prepared by dissolving them in 30 mL methanol. The pH of the solution was altered by gradually introducing glacial acetic acid. The solution was refluxed at 60^{0}C for 5–6 h before being progressively cooled. A yellow-coloured precipitate was produced, which was filtered, cleaned, and dried. The precipitate is soluble in hot DMF. The yield obtained was 66 % (2.3 g). Recrystallisation was done using DMSO but the crystal obtained was not suitable for X ray diffraction.

3.1. Invitro antimicrobial studies

The synthesized compound is subjected to invitro-antimicrobial studies using Agar well diffusion method. The analysis is carried out using two Gram positive bacteria (*S.aureus, B. subtilis*), two Gram negative bacteria (*E.coli, P. aeruginosa*). Antifungal analysis is carried out in two fungi (*C.Albicans, A. Niger*) [][][] [18,19] [][][].

3.2. Invitro anticancer studies

The compound's anticancer activity was evaluated against the human breast cancer cell line MCF-7 using the MTT assay. The cell line was procured from the National Centre for Cell Sciences (NCCS), Pune, India. The cells were cultured in Dulbecco's Modified Eagles Medium (DMEM-Himedia), supplemented with 10 % heat inactivated Fetal Bovine Serum (FBS) and 1 % antibiotic cocktail containing Penicillin (100 U/ml), Streptomycin (100 μg/mL), and Amphotericin B (2.5 μg/mL).

3.3. Molecular docking studies

Molecular docking is a computer modelling technique, which makes it easier to anticipate better orientation of the ligand with the selected protein. It is a computer aided drug design which can contribute a lot to the pharmaceutical industries. Docking studies of the ligand is carried out in CB Dock with various receptor proteins to identify various binding sites. The proteins were obtained from Protein Data Bank.

4. Result and discussion

4.1. DFT computational method

4.1.1. Geometry optimization

The geometry of the synthesized ligand BNH was optimized by using B3LYP/6–311++G (d, p) with accuracy and is shown in Fig. 1. Maximum force $= 8 \times 10^{-06}$, RMS force $= 1 \times 10^{-06}$, Maximum displacement $= 0.000682$, RMS displacement $= 0.00015$, predicted energy change $= -8.609998 \times 10^{-10}$ Hartree are the convergence limits. The $C_7 = N_{15}$ bond length is 1.2977 A^0 and that of $N_{16} - C_{17}$ length is 1.387 A^0. The bond length of $N_{16} - C_{17}$ is slightly greater than that of $C_7 = N_{15}$, due to the shorter bond distances of double bond than single bond. Similar is the case of $C_8 = N_{24}$ and $N_{25} - C_{26}$. $C_8 = N_{24}$ has a bond distance of 1.2969 A^0 and the bond distance of $N_{25} - C_{26}$ is 1.391 A^0. $N_{15} - N_{16}$ and $N_{24} - N_{25}$ shows almost equal bond distances of 1.3428 A^0 and 1.3538 A^0 respectively. Also, both the carbonyl groups $C_{17} = O_{33}$ and $C_{26} = O_{34}$ have bond lengths of 1.2207 A^0 and 1.2187 A^0 respectively. $C_{21} = N_{22}$ has a bond length of 1.3362 A^0 which is similar to the bond length of $C_{28} = N_{29}$ having value of 1.3338 A^0. Both this C=N belongs to the pyridine ring of the nicotinic hydrazide. The bond angle of $C_7 - C_8 - N_{24}$ has a value of 117.3325^0. $N_{24} - N_{25} - H_{50}$ shows a bond angle of 120.3121 A^0 which is similar to $N_{15} - N_{16} - H_{45}$ having an angle of 120.1104^0. Both $N_{16} - C_{17} - O_{33}$ and $N_{25} - C_{26} - O_{34}$ exhibits similar bond angle of 118.2036^0 and 118.3395^0 respectively. Similarly, $C_{21} - N_{22} - C_{23}$ and $C_{28} - N_{29} - C_{30}$ also have almost similar values of 117.8331^0 and 117.6592 respectively.

The dihedral angles of $H_{45} - N_{16} - C_{17} - O_{33}$ is 6.7456^0, $H_{37} - C_3 - C_4 - C_7$ is 1.9181^0, $N_{15} - N_{16} - C_{17} - C_{18}$ is 8.4034^0, C8– $N_{24} - N_{25} - H_{50}$ is 9.4188^0 and $H_{50} - N_{25} - C_{26} - O_{34}$ is 1.1056.
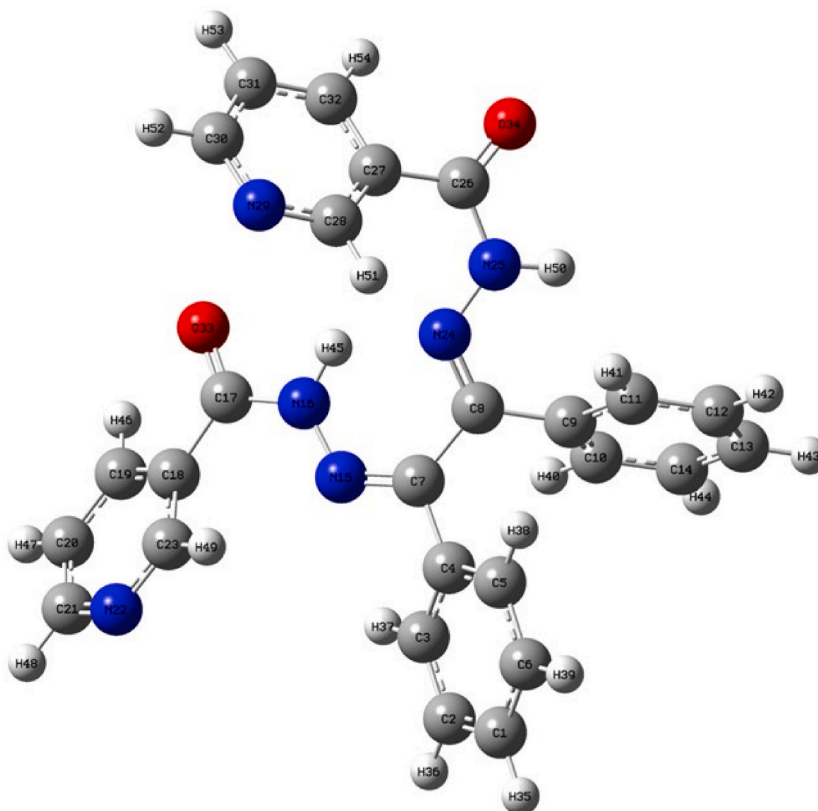

Fig. 1. Optimized geometry of BNH.

4.2. Mass analysis

The calculated molecular weight and fragmentation process of the ligand are determined by its mass spectrum. In accordance with the indicated molecular weight of the ligand $[C_{26}H_{20}N_6O_2]$ +, the pattern exhibits a parent molecular ion peak at ($m/z = 449$ amu) which also represents the base peak. Due to the progressive breakdown of the ligand, various peaks were seen. A peak at $m/z = 326$ shows $[C_{21}H_{16}N_3O]+$ due to the loss of $C_5H_4N_3O$. A second fragment $[C_{14}H_{11}N_3O]+$ with a m/z of 237 results from the loss of C_6H_5, the base peak of the spectrum. Another fragment at $m/z = 223$ $[C_{13}H_9N_3O]$ + by losing one of the CH moiety. This result makes clear evidence of the proposed molecular formula ($C_{26}H_{20}N_6O_2$) of the ligand.

4.3. Experimental and theoretical analysis

4.3.1. ^1H NMR and ^{13}C NMR

Using TMS as the internal standard, ^1H NMR and ^{13}C NMR of BNH is analyzed in DMSO solution. ^{1}HNMR of the ligand shows the aromatic protons whose peaks ranges from 7.44 to 7.93 ppm [20]. Another peak at 8.59–8.69 ppm indicates the presence of azomethine hydrogen (HC=N) [21]. Peak at 11.6 represents NH group present in the compound [22]. A sharp singlet at 3.35 ppm indicates the presence of methylene group in the ring [23]. The peak at 2.4–2.5 ppm due to the protons of DMSO [24]. In ^{13}CNMR, a minor peak at 163.9 ppm is that of the C=O carbon [25]. 123.7–138 ppm represents aromatic carbon of the ligand. Another peak at 149.1 ppm shows carbon atom (C=N) azomethine groups [26,27]. Peak at 152.5 ppm indicating the C–N carbon atom [27] and 39.35–40.6 ppm indicates carbon atoms of DMSO [28].

Theoretical calculations of the ^{1}HNMR also show peaks at 6-7.5 range shows aromatic hydrogen in the ligand. Azomethine hydrogens comes between 8 and 8.5. Peak around 10.04 ppm indicates NH hydrogen present. In ^{13}C NMR, carbon atom of C=O moiety is represented by 166.37 ppm and 166.45 ppm. Peak around 149 ppm shows azomethine carbon atom (C=N). Aromatic carbons are represented by 120ppm-135 ppm. Another peak around 150 ppm indicates C–N carbon atom of the pyridine ring. Experimental results are in agreement with the theoretical analysis which supports the structure proposed above.

4.4. FT IR analysis

The weak band in the region 3270-3160 cm^{-1} show in the spectrum of the synthesized ligand is attributed to v (N–H) [29]. It is a broad peak which indicates the presence of hydrogen bond of the type NH …. N [30]. A low intensity band between 3080 and 3000 cm^{-1} represents aromatic ν(C–H) [31]. There is a sharp peak at 1664 cm^{-1} which is due to the presence of C = 0 group of the ligand. C=N $_{hyd}$ N stretching vibrations are shown by sharp peaks around 1530 cm^{-1} [32]. Vibrational frequencies between 1560 cm^{-1} and 1417 cm^{-1} exhibits the presence of ν(C=N) and ν(C=C) bonds of the two-pyridine ring and aromatic ring respectively [29,33]. Also, there is a N–N bond vibrations around 1023 cm^{-1}. There is a presence of deformation vibration of C–H aromatic bond between 833 cm^{-1} and 730 cm^{-1} [34].

IR intensities of the BNH is computed by using B3LYP/6–311++G (d, p). A weak band in the region of 3349 cm^{-1} indicates the presence of v (N–H). Similar to experimental analysis, a sharp peak is observed at 1663 cm^{-1} in theoretical calculation also, due to the presence of C=O group of the ligand. Frequency around 1516 cm^{-1} exhibits the presence of ν(C=N) which is varied from the experimental observation. C–H deformation can be identified around 924 cm^{-1}. This shows that the theoretical observation is in agreement with the experimental one which contributes to the structure proposed by mass analysis (Fig. 2).

4.5. UV interpretation

Using a DOUBLE BEAM UV-VIS Spectrophotometer: 2202, the ligand's UV absorbance spectrum was captured over the wavelength
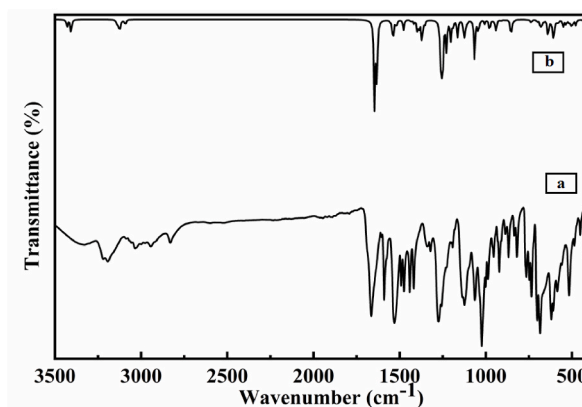

Fig. 2. IR spectrum – a) Experimental and b) Theoretical.

range of 200–700 nm using ethanol as solvent. Typically, the bands at 300–400 nm in the UV–vis spectrum of Schiff base compounds represent the excitation of electrons of the azomethine C=N group [35]. High intensity bands in this spectrum around 350–360 nm were attributed to the n- π*transitions of C=N [36]. While performing experimental calculation of BNH, the intensity peak is observed at 357 nm point out the presence of the n- π* transition of C=N azomethine group [37]. Theoretical calculation is done using DFT study which shows a broad spectrum with an intensity peak of 351 nm Fig. 3. Both experimental data are consistent with theoretical data which clearly give evidences for the structure of BNH.

Noncovalent interactions like hydrogen bonding, π-π interactions can be obtained from UV–Vis spectra of BNH. The theoretical band is observed at 351 nm, and the experimental at 357 nm. This shift can be attributable to the effect of ethanol used which changes the UV–Vis spectrum. H bonding interactions produce absorption band shifts, primarily by influencing the electron stretching of the ligand or altering its surroundings [38–42].

4.6. Fluorescence studies

The photoluminescence study of the ligand is observed in the 300–600 nm range Fig. 4. The emission spectrum of the ligand shows a high intensity peak at 424 nm on excitation at 357 nm. This high intensity peak is due to the intra ligand π-π* transitions exhibited by Schiff bases [43]. Also, this shows the high rigidity of the molecule. Since it exhibits high intensity peak, it can show fluorescent effects and hence can be used as photosensitizer against cancer cells thereby contributing to the cancer treatment [44].

4.7. Molecular electrostatic potential analysis

The primary emphasis of molecular electrostatic potential is the electron density, which provides details on potential sites for electrophilic and nucleophilic attack as well as hydrogen-bonding interactions. The electrophilic and nucleophilic attacking sites were identified utilising MEP analysis employing the B3LYP/6–31++G (d, p) method. The MEP is coloured red for negative charge, which indicates the likelihood of electrophilic reactivity, blue for positive charge, which suggests a possibility of nucleophilic reactivity, and green for neutral. The quantification of a molecule's electrostatic potential also makes it possible to determine its biological reactivity, especially when it comes as a drug receptors and enzyme-substrates interaction. Lone pairs of electronegative atoms are typically linked to negative potential regions [45–47].

From the MEP plot of BNH, the positive region is mainly localised on the Schiff base group, one of the phenyl rings of benzene and pyrimidine ring of nicotinic hydrazide. These are more prone to nucleophilic attack. The negative region concentrates on the one of the phenyl ring of the benzil, where electrophilic attack occurs. Remaining area shown by green colour indicates zero potential and small yellow portion indicates slightly electron rich regions (Fig. 5).

4.8. Frontier Molecular orbital analysis (FM0)

The lowest occupied molecular orbital (LUMO) and the highest occupied molecular orbital (HOMO) are taken into account while performing an FMO analysis of the ligand. The electron distribution in the orbitals, their energies, the energy gap between them, chemical hardness, electronegativity, and ionisation energies were all calculated using the FMO analysis [48] which is shown in Fig. 6. Determining the energy gap provides information on the electrical and optical properties of molecules as well as the chemical reactivity of the ligand. Lower the energy gap, more predominant will be the possibility of excitation of electrons and higher will be the reactivity. Also, more the FMO energy gap, the molecule is less reactive and more stable which makes it harder and vice-versa [49]. Here the orbitals that were examined include HOMO and LUMO, which are thought to be the key orbitals involved in electron transfers in chemical reactions [50,51]. HOMO of the ligand is mainly located in one of the aromatic rings of the benzil and the C=O–NH–N=CH moiety of benzil and nicotinic hydrazide whereas in LUMO electron density move towards aromatic ring of the
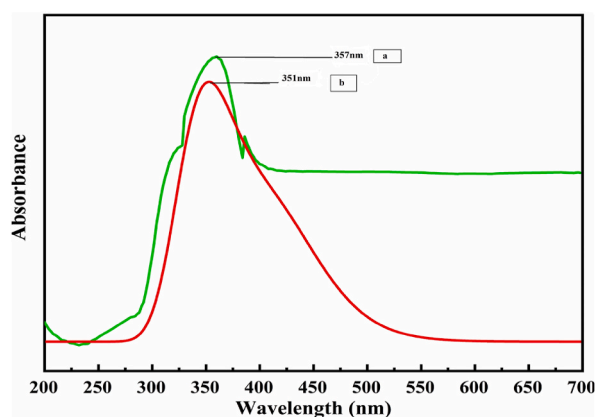

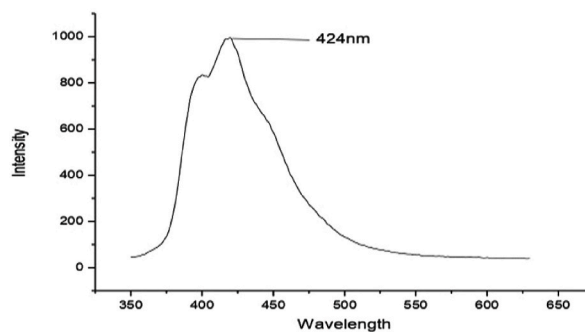**Fig. 3.** UV spectra of BNH(a)Experimental (b) Theoretical.

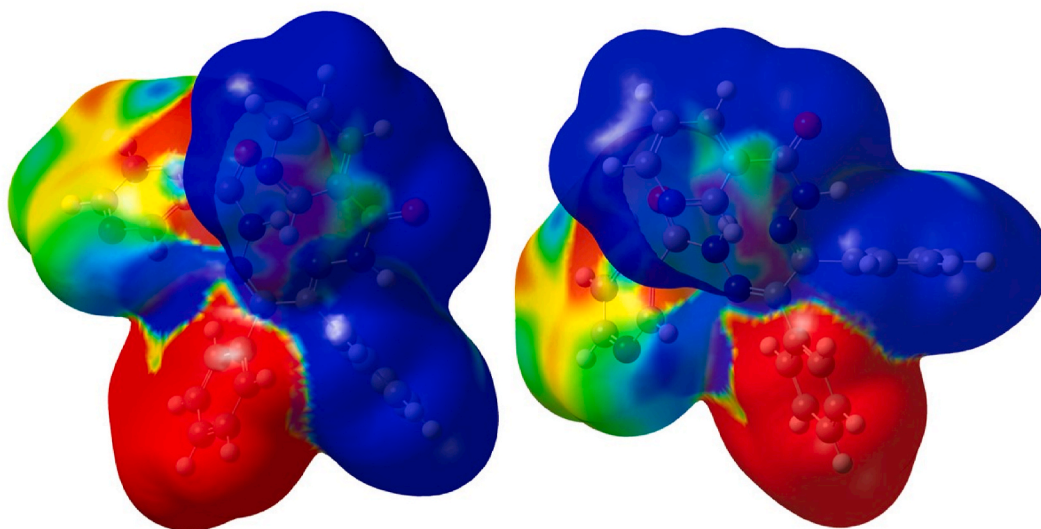**Fig. 4.** Fluorescence spectrum of the synthesized ligand.

Fig. 5. MEP Plot of the ligand.

benzil, one of the pyridine rings of nicotinic hydrazide and to C=O–NH–N=CH moiety. Here the energy for HOMO = −6.4052eV and LUMO = −2.4978eV. The Ionisation energy of the compound, I = -E_{HOMO} = 6.4052eV and Electron affinity(A) = -E_{LUMO} = 2.4978eV. From this, various chemical parameters, Electronegativity (χ) = (I + A)/2 = 4.451eV. Chemical potential(μ) = -(I + A)/2 = −4.451eV. Global hardness(η)= (I-A)/2 = 1.954eV. Global Softness = 1/η = 0.5117eV, which is the reverse of global hardness, Electrophilicity index (ω) = μ^2/2η = 5.0694 eV can be calculated. The energy gap between HOMO-LUMO = 3.9071 eV.

4.9. Mulliken charges

Mulliken charge calculation of a given molecule allows one to identify the atomic ions within. This alters the vibrational spectrum, which in turn has an effect on a variety of other aspects of the system, including bond lengths of the atom, their dipole moments, molecular polarizability, their electronic structures, their acidity-basicity characteristics etc. The figure displays the calculation of Mulliken atomic charges using the DFT method [52,53]. All hydrogen atoms present in the molecule possess net positive charges. H45 has the highest positive charge among all other hydrogens with a value of 0.522. Oxygen atoms O33 and O34 has negative charges of −0.177 and −0.196. Nitrogen atoms N22 and N29 which are a part of the heterocyclic aromatic rings possess positive values. Nitrogen N15 connected to C7 and N24 connected to C8 which forms C=N group possess positive values. But nitrogen N16 and N25 of CO–NH–N=CH possess negative values of −0.060 and −0.066. The carbons C3, C4, C9, of the benzil ring and C18, C19, C27 and C32 of the nicotinic hydrazide ring, found to have net positive charges. Among the positive carbons, C18 attached to C=O group has high positive charge of 0.962 which shows its acidic nature. Hence nucleophilic attack is preferred here. C7, C8 carbon atom of the C=N group shows negative charges of −0.526 and −0.457 respectively. C17 and C26 attached to the oxygen atom also shows negative charges. High electron density at O33, O34, N25, N16, C10 (−0.197), C11 (−0.059), C21 (−0.143) indicates a possibility of electrophilic attack at these sites.
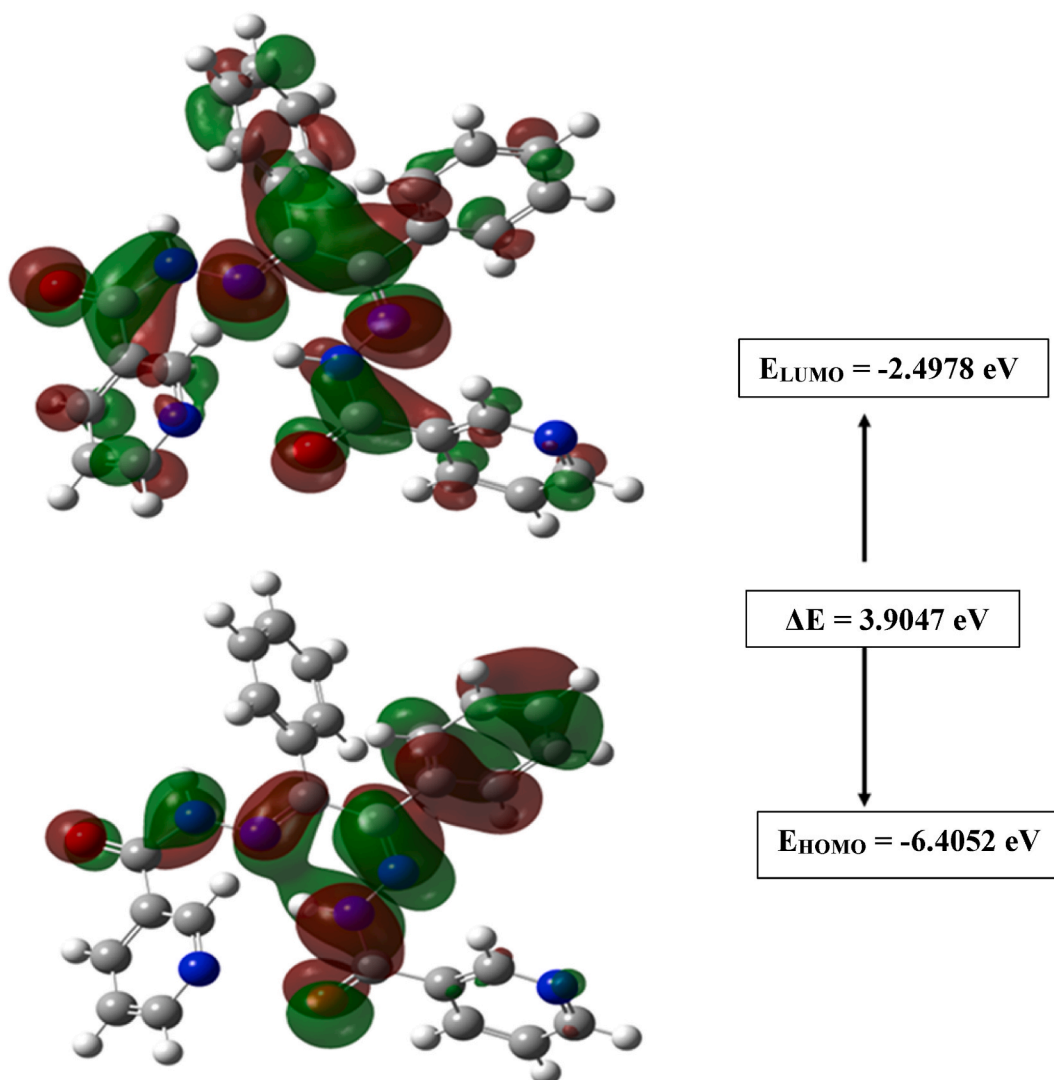
Fig. 6. HOMO- LUMO of BNH.

5. Biological studies

5.1. Antimicrobial studies

The method widely used for the evaluation of antimicrobial activity of the compound is Agar well diffusion method [54]. Muller-Hinton Agar medium (HIMEDIA-M173) is employed in antibacterial research to determine the susceptibility of microorganisms to antimicrobial agents. Two Gram positive bacteria (*S. Aureus* and *B. Subtilis)* and two Gram negative bacteria (*E.coli* and *P. Aeruginosa*) are used in the analysis. 38 g of the chemical are dissolved in 1000 cc of distilled water and heated. Bacterial cultivation is done using this medium. Distilled water is used as solvent which is used as negative control. The test samples (50 and 100 L) were added to wells T1 and T2 from the 10 mg/mL stock and plate is incubated. The standard is chosen to be *Gentamycin.* [55]. The results obtained were compared with the standard. There is no inhibition shown by *S. Aureus, E. Coli* and *P. aeruginosa* for the compound at this concentration. Also, the compound doesn't show activity greater than the standard. *Bacillus subtilis* shows some inhibition in this concentration but the value is not greater than the standard value Fig. 7.

Antifungal analysis is carried out in two fungi (*Candida Albicans, Aspergillus Niger*) [][][] [56] [][][] (see Table 1). Mueller-Hinton agar and Potato Dextrose Agar MH096 Himedia was used to test the sensitivity of different fungi strains to antifungal drugs [57]. Fungal suspension was made in this medium. Standardized inoculum was evenly dispersed around the plate. The test samples (50 and 100 L) were introduced to wells T1 and T2 and incubated. *Clotrimazole* is selected as the standard [58]. While comparing the results obtained with those shown by various Schiff bases, the synthesized BNH is less active towards selected bacteria and fungi. The activity of the synthesized compound is lesser than that of the standard. The compound is inactive since the zone of inhibition observed is
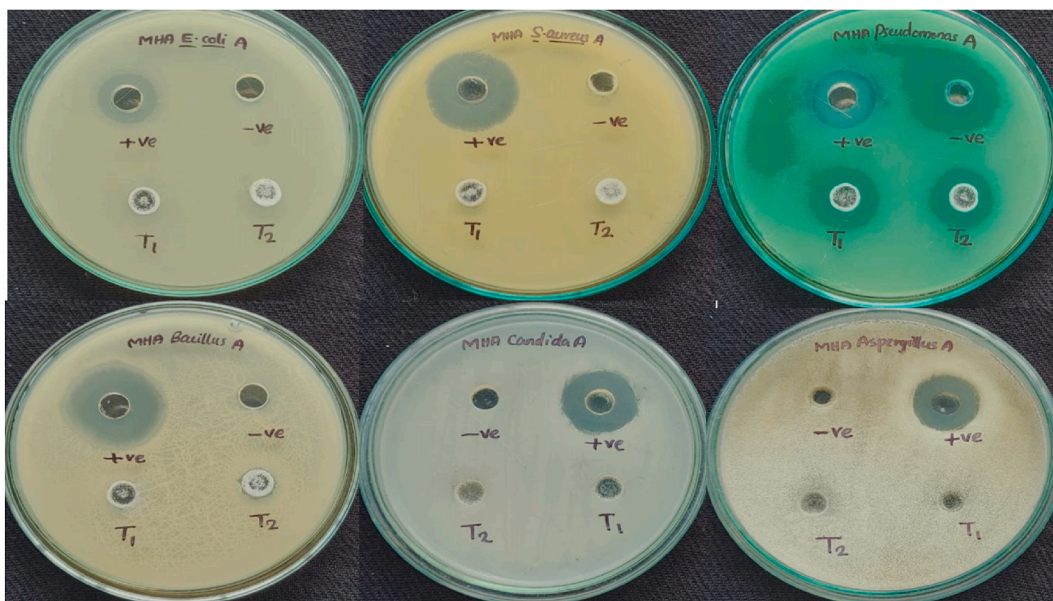
Fig. 7. Zone of inhibition of Bacteria and Fungi.

negative and there is no inhibition at this concentration (Table 2.). Even though BNH shows negative zone of inhibition against selected microorganisms, it can be used as a carrier for drug in drug delivery studies.

5.2. In vitro anticancer study

Invitro anticancer study of the compound was assayed by MTT assay against MCF-7(Human Breast cancer cell line). MTT assay or (3-(4,5-dimethylthiazol-2-yl)-2,5-diphenyltetrazolium bromide is used to measure the cytotoxicity of the Schiff base ligand. The cells (2500 cells/well) were planted on 96-well plates and they were given time to adjust to the culture condition. The DMEM media (10 mg/mL) was used to create test samples. The samples were added to the grown cells having different concentrations of 6.25,12.5,25,50 and 100 g/mL and incubated. 100 mL of a 0.5 mg/mL MTT solution in PBS is added to the wells and again incubated. Finally 100 mL of 100 % DMSO were added to each well and finally the absorbance was measured at 570 nm. Here DMSO is used a a negative control for the analysis. The IC$_{50}$ value (the dose blocking 50 % of growth relative to the viability control) is a key factor in determining cytotoxicity [59].

The ligand shows cytotoxicity against all the three cell lines tested. The ligand shows cytotoxicity against MCF-7 human breast cancer cell (IC$_{50}$ value of 45.58) and A549 human lung cancer cell (IC$_{50}$ value 51.19). This shows that the synthesized compound has better cytotoxicity against MCF-7 human breast cancer cell than lung cancer cell. The cytotoxicity of the ligand against breast cancer cell lines significantly emphasises the importance of metallodrug design in medical inorganic chemistry (Fig. 8).

6. Molecular docking

Molecular docking is a type of computational modelling that makes it easier to anticipate the preferred binding orientation of one molecule (such as a ligand) to another (such as a receptor) when they combine to form a stable complex [60]. Molecular docking was

Table 1
Thermochemical Data from DFT analysis.

Thermal Energy	1163.0222 kJ/mol
Heat capacity (Cv)	*0.453661 kJ/mol*
Entropy (S)	*0.824293 kJ/mol*
Electronic energy (EE)	*−3891253.8464 kJ/mol*
Zero-point Energy Correction	*1088.8947 kJ/mol*
Thermal Correction to Energy	*1162.8786 kJ/mol*
Thermal Correction to Enthalpy	*1165.5015 kJ/mol*
Thermal Correction to Free energy	*919.9017 kJ/mol*
EE + Zero-point Energy	*−3890176.3411 kJ/mol*
EE + Thermal Energy Correction	*−3890102.0394 kJ/mol*
EE + Thermal Enthalpy Correction	*−3890099.6765 kJ/mol*
EE + Thermal Free Energy Correction	*−3890345.1608 kJ/mol*

Table 2
Zone of inhibition shown by Bacteria and Fungi.

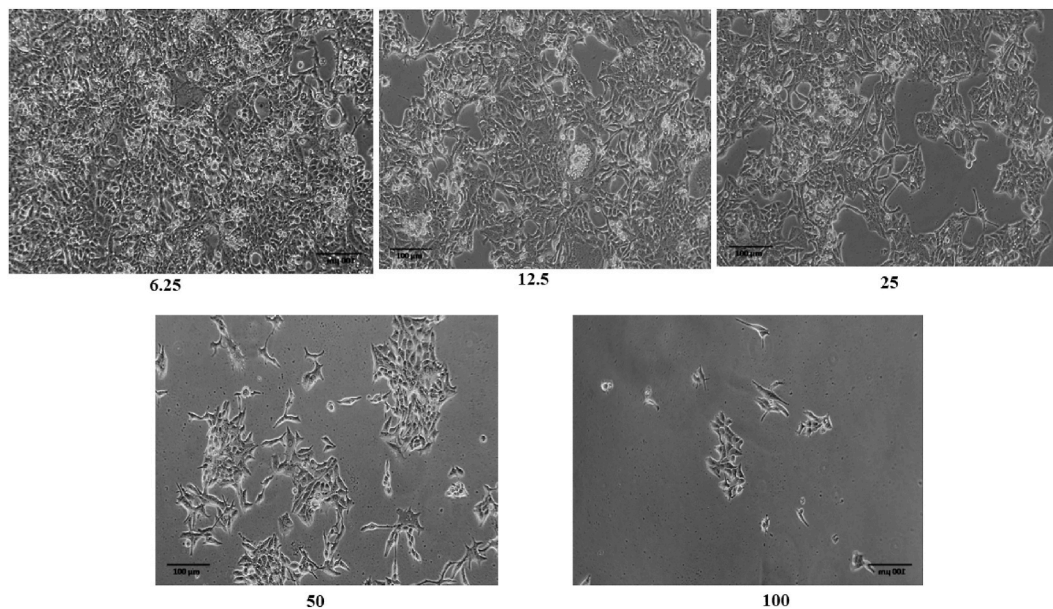| SI NO	Name of Microorganism	Zone of inhibition (mm)			
		Standard *Gentamycin*	Negative Control	T1 (500 µg)	T2 (1000 µg)
1	*E.Coli*	17 mm	-ve	-ve	-ve
2	*S Aureus*	25 mm	-ve	-ve	-ve
3	*P. Aeruginosa*	19 mm	-ve	-ve	-ve
4	*B. subtilis*	26 mm	-ve	-ve	+ve (9 mm)
5	*C. Albicans*	22 mm	-ve	-ve	-ve
6	*A. Niger*	19 mm	-ve	-ve	-ve

Fig. 8. Cytotoxicity analysis of ligand at different concentrations.

performed by the synthesized ligand with various breast cancer proteins using online databases CB Dock. The docking of the ligand and the protein is done using online database.

The CB-Dock (Cavity-detection guided Blind Docking) is a webserver utilises a unique curvature-based cavity detection approach to anticipate the binding sites of a given protein and calculate the centres and sizes. CB-Dock produces a set of points to represent the solvent-accessible surface and computes the curvature factor for each point. Docking box was customized for computation by CB-DOCK. A decent docking box encloses the native binding poses while excluding as many extraneous poses as possible. The key parameters of this process is the centre and size of the docking box [][][] [61] [][][]. Choosing a suitable center ensures that the docking calculations concentrate on the relevant area of the protein, improving the likelihood of discovering biologically meaningful binding poses. Choosing the right size means that the docking method has ample room to investigate various ligand conformations and orientations within the binding site. The server is designed to interact with AutoDock Vina and has been meticulously tuned to produce models with a success rate of more than 70 % [[62,63]. The ligand is taken in pdb format and the selected proteins is obtained in pdb format from RCSB protein data bank. Both ligand and receptor is inserted and docking is performed. The ligand usually interacts with the pharmacologically active site in the proteins. Based on the Vina score, the higher negative binding energy indicates the strongest interaction between the chosen proteins and the ligand [19]. Depending on the Vina score obtained by doing the analysis, five possible coupling cavities were identified. One of those was chosen based on its higher negative energy [64]. The binding modes obtained were shown in Fig. 9. The interactions and 2D visualisation of the proteins and ligands were then generated using BIOVIA [65]. Elements were used to configure the ligand and protein colours. The Ligplot analyses were developed to comprehend the intricate network of interactions between the docked ligands and the active site residues. Ligplot is a crucial tool for comprehending the pattern of hydrogen bonds and hydrophobic interactions [66].

By considering the role of certain target receptors in the initiation and progression of breast cancer, we selected a series of five breast cancer proteins based on the literature review and the docking is performed with the synthesized compound. The ligand's potential to interfere with the actions of the aforementioned target receptors, inhibiting their function and accelerating the progression of cancer, is the premise of the docking study [67,68]. The proteins are Progesterone Receptor (PR) (PDB ID: 1SQN) [69], Epidermal

a

Vina score	Cavity size	Center			Size		
		x	y	z	x	y	z
-8.6	636	-4	-2	39	24	24	24
-7.7	713	17	27	-4	24	24	24
-6.6	704	-7	-1	20	24	24	24
-6.5	383	11	25	8	24	24	24
-5.7	407	-3	2	25	24	24	24

b

Vina score	Cavity size	Center			Size		
		x	y	z	x	y	z
-8.3	665	24	0	54	24	24	24
-7.1	991	36	8	51	24	24	24
-6.3	184	40	18	67	24	24	24
-6	173	3	15	63	24	24	24
-5.9	416	31	-4	40	24	24	24

c

Vina score	Cavity size	Center			Size		
		x	y	z	x	y	z
-8.1	1199	0	58	55	24	24	24
-7.7	974	1	75	60	24	24	24
-7.7	910	-3	47	61	24	24	24
-7.6	1143	4	81	93	24	24	24
-7.6	1087	5	57	82	24	24	24

d

Vina score	Cavity size	Center			Size		
		x	y	z	x	y	z
-10.1	3640	-4	15	1	24	24	32
-9.9	5179	26	31	0	32	35	35
-6.3	164	13	16	14	24	24	24
-5.4	137	-20	9	3	24	24	24
-4.8	137	40	45	-3	24	24	24

e

Vina score	Cavity size	Center			Size		
		x	y	z	x	y	z
-8.8	1846	-4	-10	-29	24	24	24
-8.6	2013	14	-18	-14	24	24	24
-8	563	12	-5	-17	24	24	24
-6.2	239	23	-29	-37	24	24	24
-5.9	246	1	-28	-19	24	24	24

Fig. 9. Vina scores obtained for a) 1SQN, b) 1M17 c) 6R3S d) 4DRH e)5NWH.

Growth Factor Receptor (PDB ID: 1M17) [70], Cyclin Dependent protein Kinase (CDK8) (PDB ID: 6R3S) [71], Mammalian Target of Rapamycin mTOR (PDB ID: 4DRH) [72] and NUDT5 signalling protein (PDB ID:5NWH) [73] (Fig. 9). After docking of the selected proteins and ligand, lowest binding energy is selected (see. Fig. 10).

The synthesized ligand and the selected protein Progesterone receptor protein (1SQN) are docked and the it shows a minimal binding energy of −8.6 kcal/mol. From the result, we can see that the GLU 695 forms hydrogen bond with hydrogen atom attached to N and O atom with distance of 2.91 and 2.95 respectively. Gln 815 shows van der Waals interaction with oxygen atom of the C=O group with distance of 2.84. LYS 822 shows interaction with oxygen atom of the C = 0 group with bond distance of 2.97. GLN 725, MET 759, VAL 729, SER 728 etc shows van der Waals interactions.

For EGFR protein (1M17) (binding energy of −8.3 kcal/mol) also, various favourable interactions are observed. LYS 721, ARG 817, ASN 818 exhibits conventional hydrogen bond with hydrogen bond attached to O atom with bond distance 2.87, 2.76 and 3.12 respectively and THR 830 interacts with hydrogen of NH group distance of 3.05. LEU 768, THR 766, GLU 738, THR 766 etc shows van der Waals interactions. Asp 831 shows electrostatic interactions with N of C=N and O of C–OH group with distance of 2.84 and 2.95 respectively.

CDK8 proteins (6R3S) (binding energy of −8.1 kcal/mol), Asp 173 show an electrostatic interaction with N of C=N and also forms hydrogen bond with NH and OH groups of the ligand. ALA97, ALA172, LYS 52 PHE 97, ALA 95 etc forms Pi Alkyl interaction with aromatic rings present in the compound.

In the case of mTOR protein (4DRH) (having binding energy of −10.1 kcal/mol), VAL 86, TRP 90, PHE 130, PHE 77, ILE 87 shows Pi-Pi stacking interactions with aromatic ring of the ligand. SER 118, TYR 57 and ASP 2102 show hydrogen bond with hydrogen at nitrogen atom. At the same time TYR 113 forms hydrogen bond with hydrogen atom attached to the oxygen atom. PHE 2039 Pi-Alkyl interaction with the aromatic ring of the compound. Also, TYR 2038, THR 2098, TYR 2105 exhibits a van der Waals interaction with aromatic rings of the system. Finally, NUDT5 (5NWH) (Binding energy −8.8 kcal/mol) show various interactions like Hydrogen bonding, Pi-Pi stacking interactions etc. Two hydrogen atoms associated with OH group of the ligand forms conventional hydrogen bond ALA 96 and GLN 82. NH_2 group of ARG 84 interacts with O of the OH group again by hydrogen bonding with a bond distance of 3.11. TRP 28, TRP 46 and LEU 98 shows Pi - Pi interaction with the phenyl rings. TRP 46 shows Pi-Pi interactions with one of the phenyl rings and the pyridine ring of the ligand.

Since the ligand and protein shows better interactions, it is clear from the docking that synthesized ligand has a better affinity for the selected proteins. Hence the synthesized compound has better activity in drug designing against breast cancer.
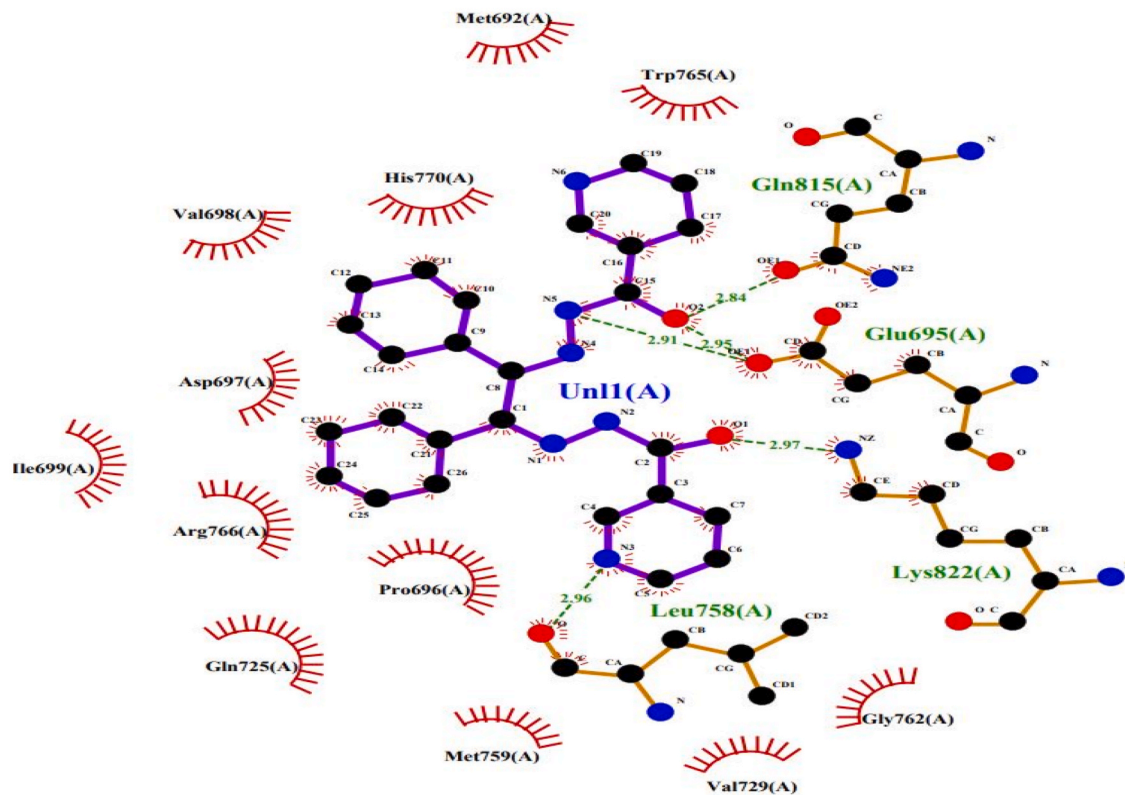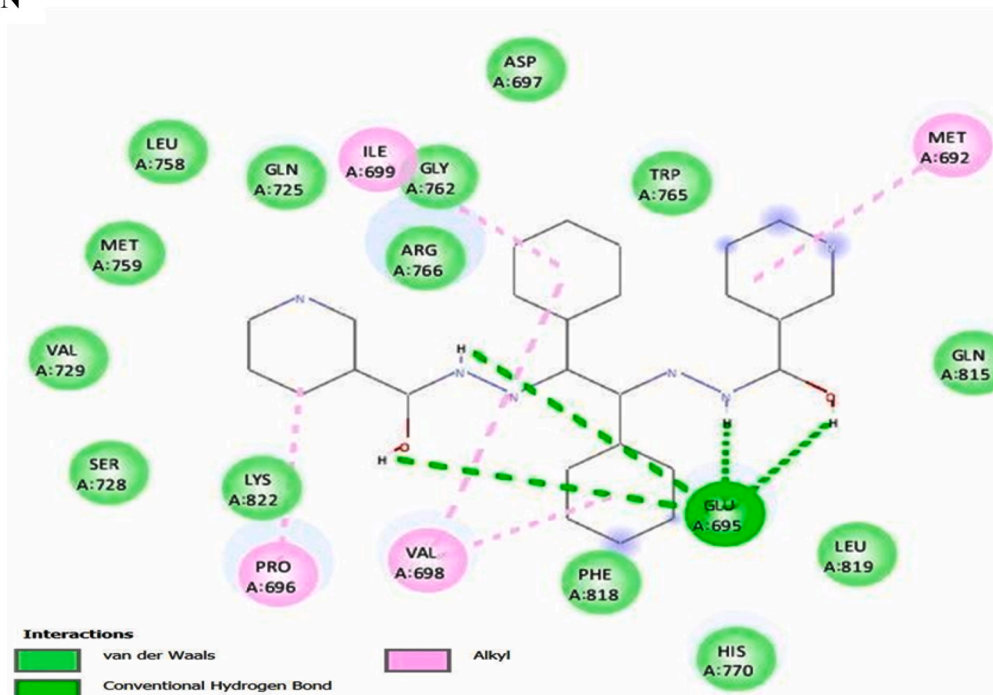
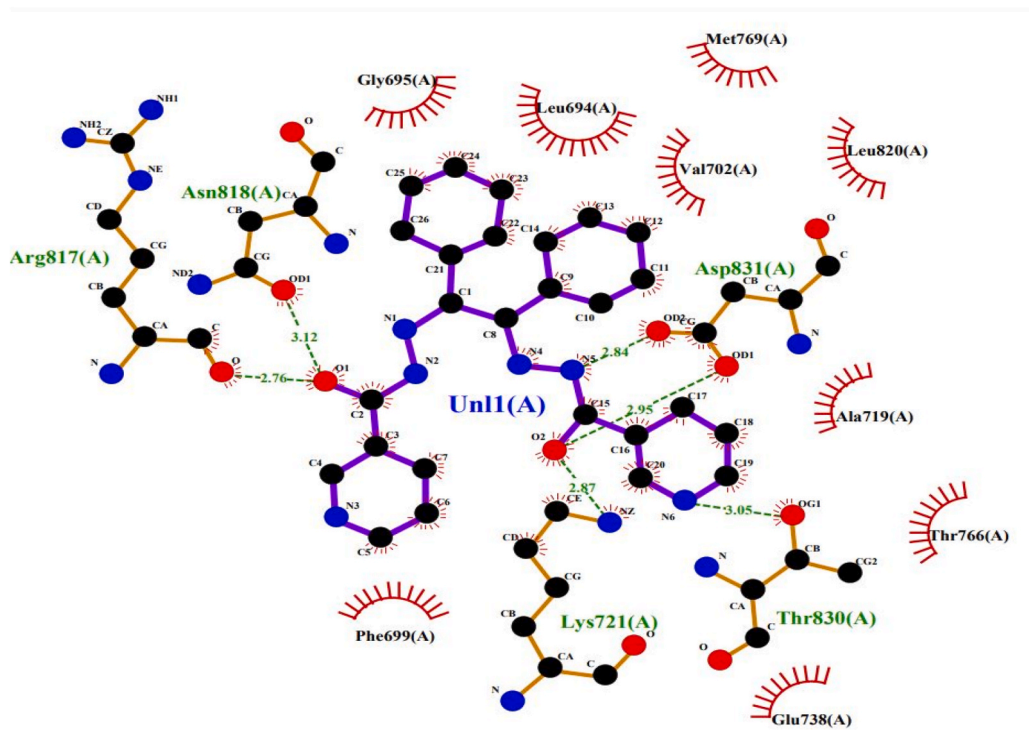**1SQN**
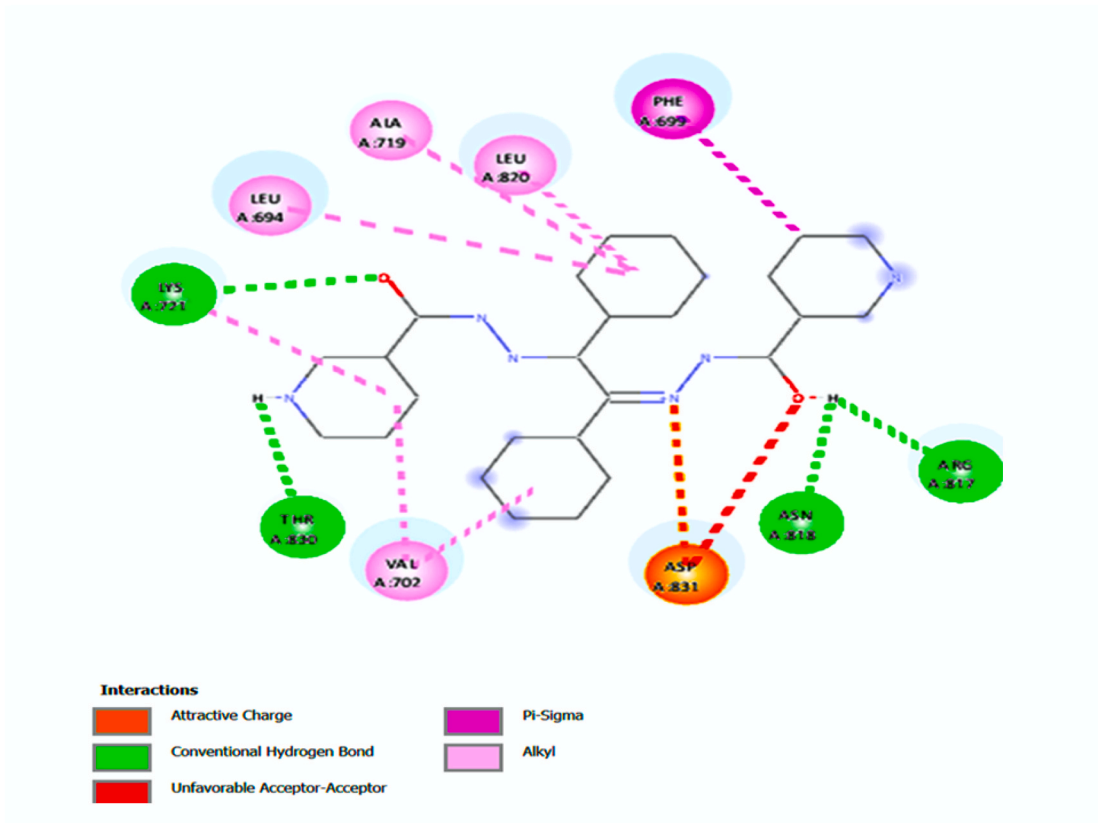

Fig. 10. Interactions of proteins with BNH.
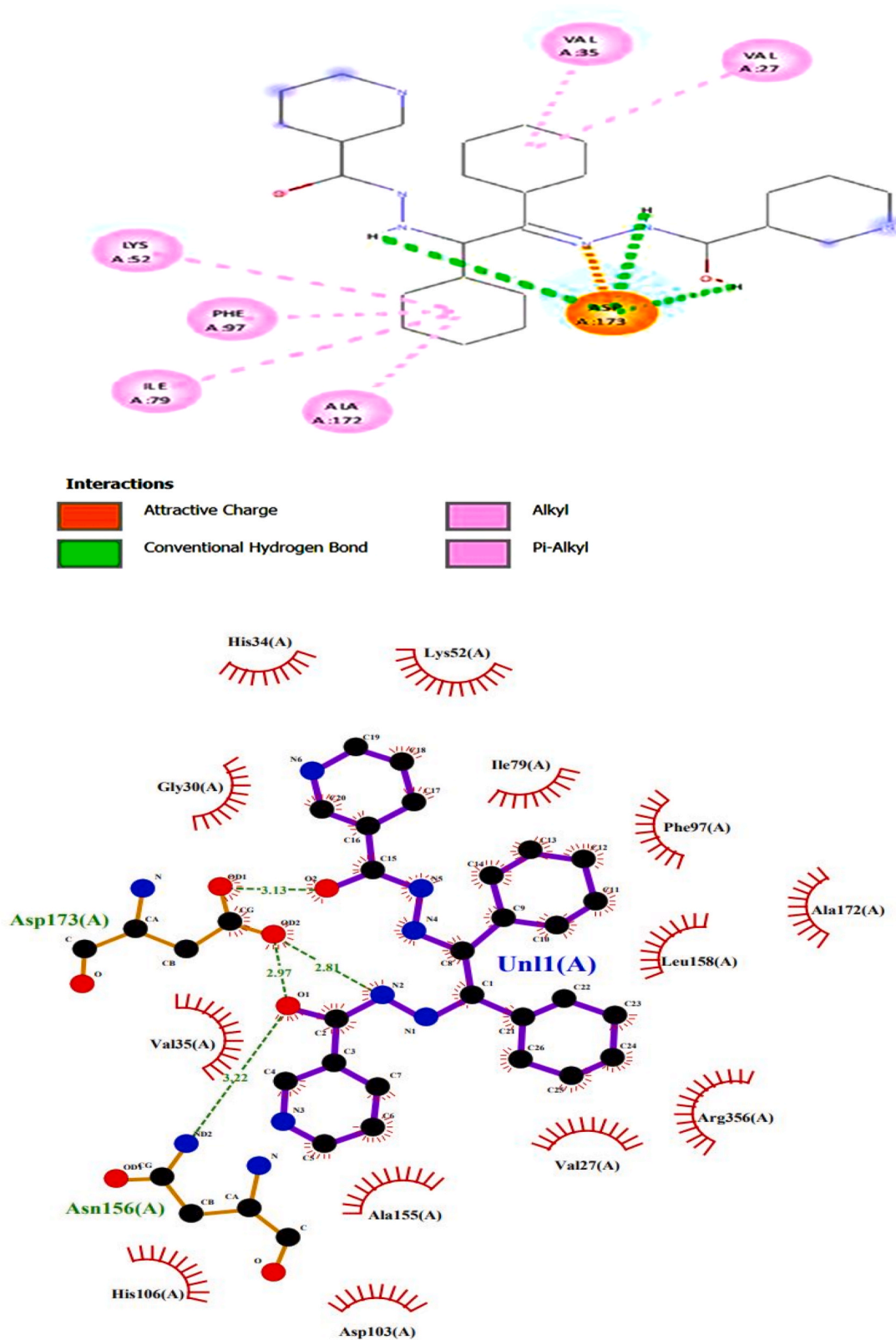
1M17

Fig. 10. (*continued*).

6R3S

4DRH
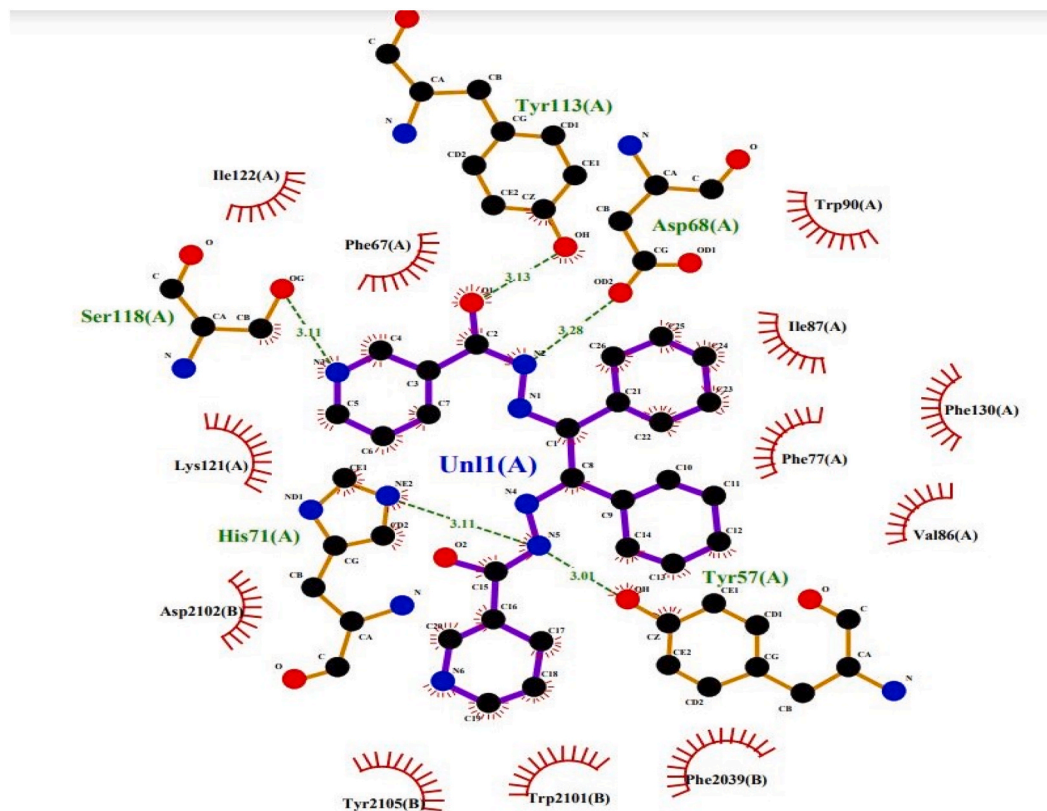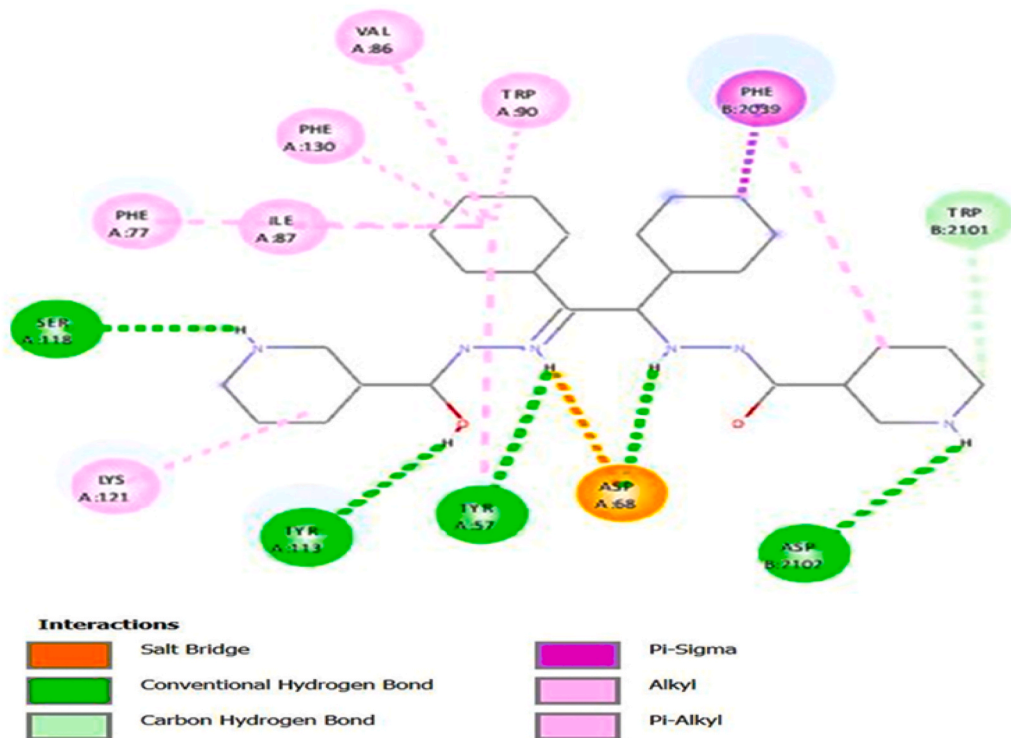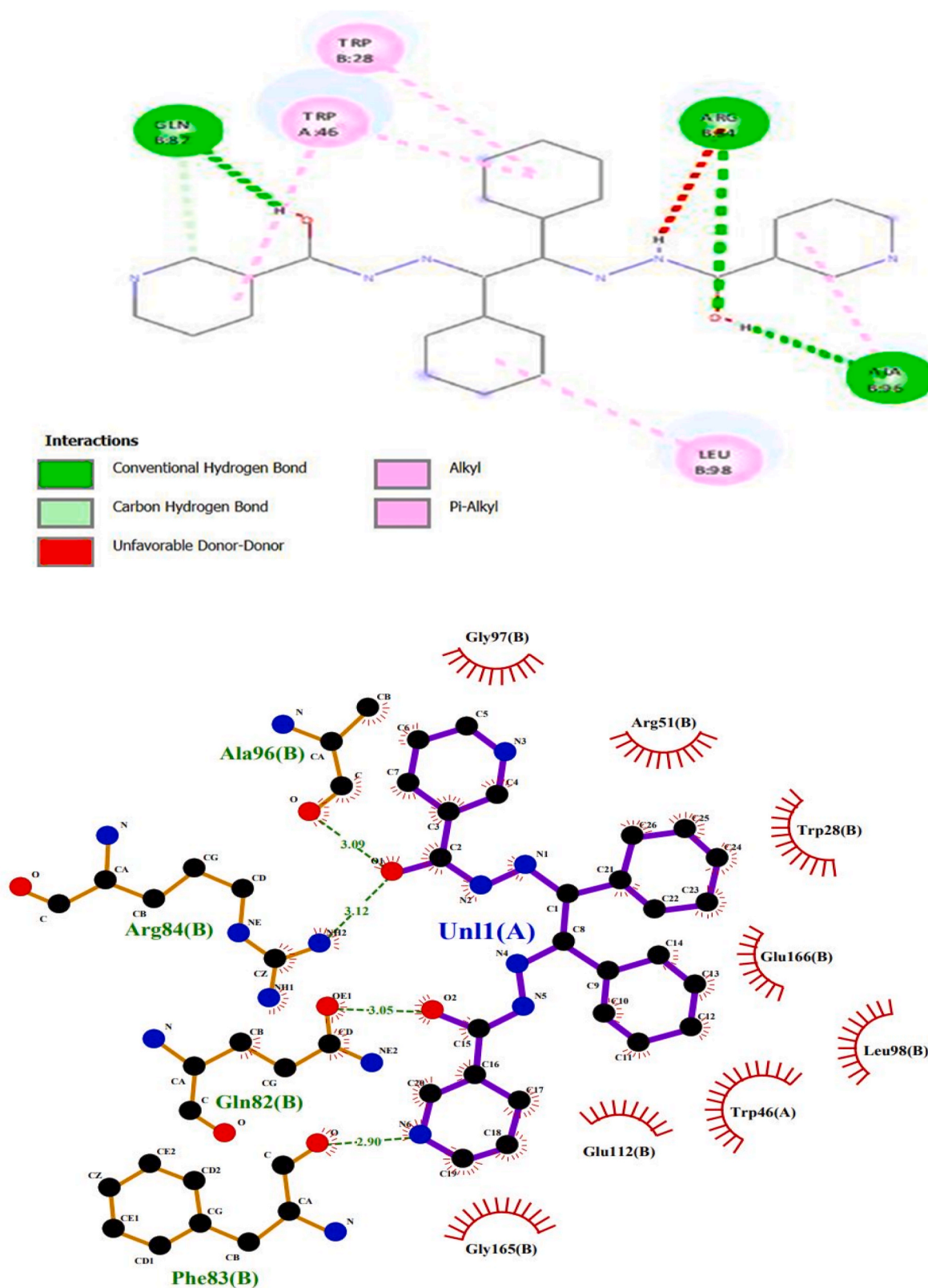

Fig. 10. (*continued*).

5NWH

Fig. 10. (*continued*).

7. Conclusions

The compound synthesises BNH from Benzil and Nicotinic hydrazide is successfully done. It is characterized by various spectroscopic techniques like FT-IR, UV, ^{1}H NMR, ^{13}CNMR, Fluorescence study and Mass spectrum. The structure of the synthesized compound was proposed by mass spectra. All other characterization techniques, both theoretical and experimental, clearly supports the proposed structure of BNH. Invitro antimicrobial studies shows that the compound is less active against the bacteria and fungi, but it can be used as a drug carrier in the medical field. By performing invitro studies of anticancer using MCF-7 cell shows that the compound is good enough for the treatment of breast cancer. Also, Molecular docking was performed with various proteins selected in the category of breast cancer and the compound has an appreciable binding energy with mTOR (4DRH) protein which point out that the BNH could be significant contribution for discovery and development of drug having anticancer effect. The findings of the in vitro research demonstrate the ability of BNH to inhibit a range of microbial activities. This property may also be utilized to create new medications for the treatment of breast cancer, which would be a significant advancement in the pharmaceutical industry. Complexes of the BNH with metals are under investigation and its applications has to be explored further for better advancement in drug discovery.

CRediT authorship contribution statement

V. Preethi: Writing – original draft, Resources, Methodology, Investigation, Formal analysis, Data curation. **V.G. Vijukumar:** Validation, Supervision, Software, Resources, Conceptualization. **S. AnilaRaj:** Methodology, Investigation, Formal analysis, Data curation. **V.G. Vidya:** Writing – review & editing, Supervision, Resources, Project administration, Methodology, Conceptualization.

Declaration of competing interest

The authors declare that they have no known competing financial interests or personal relationships that could have appeared to influence the work reported in this paper.

Appendix A. Supplementary data

Supplementary data to this article can be found online at https://doi.org/10.1016/j.heliyon.2024.e29689.

References

[1] Bhupender S. Chhikara, Keykavous Parang, Global Cancer Statistics 2022: the trends projection analysis, Chemical Biology Letters 10 (1) (2023) 451.
[2] Adnan Taleb Nasser, Rafid Humaidan Al-Asadi, Schiff bases ligands derived from o-phthalaldehyde and their metal complexes with Cu2+ and Ni2+: synthesis, anti-breast cancer and molecular docking study, Trends in Sciences 20 (9) (2023) 5675.
[3] Beata Smolarz, Anna Zadrozna Nowak, Hanna Romanowicz, Breast cancer—epidemiology, classification, pathogenesis and treatment (review of literature), Cancers 14 (2022) 2569.
[4] Dharambir Kashyap, Deeksha Pal, Riya Sharma, Vivek Kumar Garg, Neelam Goel, Deepika Koundal, Atef Zaguia, Shubham Koundal, andAssaye Belay, Global increase in breast cancer incidence: risk factors and preventive measure, Hindawi BioMed Research International (2022) 16. Article ID 9605439.
[5] S. Arulmurugan, Helen P. Kavitha, B.R. Venkatraman, Biological activities OF SCHIFF base and its complexes: a review, Rasayan J. Chem. 3 (3) (2010) 385–410.
[6] Sadia Afrin Dalia, Farhana Afsan, Md Saddam Hossain, Md Nuruzzaman Khan, C.M. Zakaria, Md Kudrat-E-Zahan, Md Mohsin Ali, A short review on chemistry of schiff base metal complexes and their catalytic application, Int. J. Chem. Stud. 6 (3) (2018) 2859–2866.
[7] Jyoti Subhash, Ashu Chaudhary, Synthesis, spectroscopic characterization, in vitro cytotoxic, antimicrobial and antioxidant studies of Co(II) complexes bearing pyridine-based macrocyclic ligands with density function theory (DFT) and molecular docking investigations, Res. Chem. Intermed. 49 (2023) 4729–4758.
[8] Garima Matela, Schiff bases and complexes: a review on anti-cancer activity, Anti Cancer Agents Med. Chem. 20 (2020) 1908–1917.
[9] Jyoti Subhash, Anita Phor, Ashu Chaudhary, Synthesis, structural elucidation, cytotoxic, antimicrobial, antioxidant, density functional theory and molecular docking studies of mononuclear Ru (II) complexes of N4O4-bearing macrocyclic ligands, J. Inorg. Organomet. Polym. Mater. 34 (2024) 827–847.
[10] Noureddine Olfa, Noureddine Issaoui, Sofian Gatfaoui, Omar Al-Dossary, Houda Marouani, Quantum chemical calculations, spectroscopic properties and molecular docking studies of a novel piperazine derivative, J. King Saud Univ. Sci. 33 (2021) 101283.
[11] Mouna Medimagh, Noureddine Issaoui, Sofian Gatfaoui, Omar Al-Dossary, Aleksandr S. Kazachenko, Houda Marouani, MarekJ. Wojcik, J. King Saud Univ. Sci. 33 (2021) 101616.
[12] Hela Habli, Leila Mejrissi, Noureddine Issaoui, Saud Jamil Yaghmour, Brahim Oujia, Florent Xavier Gadea, Ab initio calculation of the electronic structure of the strontium hydride ion (SrH1), Int. J. Quant. Chem. 115 (2015) 172–186.
[13] Jyoti Subhash, Monika Gupta, Anita Phor, Ashu Chaudhary, Synthesis, spectral characterisation, in vitro cytotoxicity, antimicrobial, antioxidant, DFT and molecular docking studies of Ru(III) complexes derived from amide-based macrocyclic ligands, Res. Chem. Intermed. 50 (2024) 1081–1111.
[14] Aleksandr S. Kazachenkoa, Mouna Medimagh, Noureddine Issaoui, Omar Al-Dossary, Marek J. Wojcike, Anna S. Kazachenkoa, V. Angelina, Yuriy N. Miroshnokovaa, Malyar, Sulfamic acid/water complexes (SAA-H2O(1-8)) intermolecular hydrogen bond interactions: FTIR,X-ray, DFT and AIM analysis, J. Mol. Struct. 1265 (2022) 133394.
[15] Abduvakhid Jumabaev, Utkirjon Holikulov, Hakim Hushvaktov, Noureddine Issaoui, Ahmad Absanov, Intermolecular interactions in ethanol solution of OABA: Raman, FTIR, DFT, M062X, MEP, NBO, FMO, AIM, NCI, RDG analysis, J. Mol. Liq. 377 (2023) 121552.

[16] Safinaz H. El-Demerdash, Shimaa Abdel Halim, Ahmed M. El-Nahas, Asmaa B. El-Meligy, A density functional theory study of the molecular structure, reactivity, and spectroscopic properties of 2-(2-mercaptophenyl)-1-azaazulene tautomers and rotamers, Sci. Rep. 13 (2023). Article number: 15626.

[17] Ravikanta, Sulekh Chandraa, Synthesis, spectroscopic investigation and in vitro fungicidal action of novel Schiff's base ligand and its metal chelates, IJPAC 13 (3–4) (2018).

[18] Ashu Chaudhary Subhash, Manish Kumar Jyoti, Ritu Solanki Mamta, Synthesis, structural elucidation, DFT investigations, biological evaluation and molecular docking studies of tetraamide-based macrocyclic cobalt (II) complexes, J. Iran. Chem. Soc. 20 (2023) 2339–2362.

[19] Ashu Subhash, Jyotimanish kumar Chaudhary, Naveen Kumar, Neeraj K. Agarwal, Synthesis, spectroscopic characterization, biocidal evaluation molecular docking & DFT investigation of 16-18 membered macrocyclic complexes of cobalt (II), J. Chem. Sci. 134 (2022) 113.

[20] W. Dikio Charity, Ikechukwu P. Ejidike, Fanyana M. Mtunzi, Michael J. Klink2, Ezekiel D. Dikio, Hydrazide SCHIFF bases of acetylacetonate metal complexes: synthesis, spectroscopic and biological studies, Int. J. Pharm. Pharmaceut. Sci. 9 (12) (2017). ISSN- 0975-1491.

[21] Kargar Hadi, Kaka-Naeini Azar, Fallah-Mehrjardi Mehdi, BehjatmaneshArdakani Reza, Hadi Amiri Rudbari, Khurram Shahzad Munawar, Oxovanadium and dioxomolybdenum complexes: synthesis, crystal structure, spectroscopic characterization and applications as homogeneous catalysts in sulfoxidation, J. Coord. Chem. 74 (2021) 9–10.

[22] Meman Sahu, Amit Kumar Manna, Kalyani Rout, Jahangir Mondal, Goutam K. Patra, A highly selective thiosemicarbazone based Schiff base chemosensor for colorimetric detection of Cu2+ and Ag+ ions and turn-on fluorometric detection of Ag+ ions, Inorg. Chim. Acta. 508 (2020) 119633.

[23] D. Ravichandrana, M. Ranjani b, G. Prabu Sankar c, R. Shankar a, M. Karthi d, S. Selvakumar d, R. Prabhakaran b, Coumarin-Picolinohydrazone derived Schiff base as fluorescent sensor(OFF-ON) for detection of Al3+ ion: synthesis, Spectral and theoretical studies, J. Mol. Struct. 1273 (2023) 134329.

[24] AbdE1AzizSafaaE1dinH. DinaM, Etaiw, E.A. Ali, Synthesis,spectroscopic,cytotoxicaspectsandcomputationalstudyofN-(pyridine-2-ylmethylene)benzo[d]thiazol-2-amine Schiffandsomeofitstransitionmetalcomplexes, JournalofMolecularStructure 1048 (2013) 487–499.

[25] A.D. KhalajiS, Hafez Ghoran, M. Poajrova, M. Dusek, Characterization and crystalstructuresofnewschiffbasenacrocycliccompounds, J Struc Chem 56 (7) (2015) 1410–1414.

[26] Dina A. Tolan, Tahani I. Kashar, Kazunari Yoshizawa, Ahmed M. El-Nahas, Synthesis, spectral characterization, density functional theory studies, and biological screening of some transition metal complexes of a novel hydrazide–hydrazone ligand of isonicotinic acid, Appl. Organomet. Chem. 35 (2021) e6205.

[27] Wail Al Zoubi, Farouk Kandil, Mohamad Khaled Chebani, Synthesis of Macrocyclic Schiff Bases Based on Pyridine-2,6- Dicarbohydrazide and their Use in Metal Cations Extraction, Zoubi et al, Org. Chem. Curr. Res. 1 (1) (2012).

[28] Nasir Uddin Mohammad, Khandaker Sonia, Moniruzman Shaharier Amin, Sumi Wahida, Atiar Rahman Md, Rahman Sheikh Mahbubur, Synthesis, characterization, molecular modeling, antioxidant and microbial properties of some titanium(IV) complexes of schiff bases, J. Mol. Struct. 1166 (2018) 79–90.

[29] Kevin Beattie, Geeta Phadke, Jasmina Novakovic, Chapter-6, Profiles Drug Subst. Excipients Relat. Methodol. 37 (2012) 245–285.

[30] M.U. Adaji, R.A. Wuana, A.U. Itodo, I.S. Eneji, M.S. Iorungwa, Metal complexes of (E) – N1 - (2- hydroxybenzylidene) nicotine hydrazid schiff base; synthesis, characterisation and nematicidal activity, Arabian Journal of Chemical and Environmental Research 9 (1) (2022) 1–27.

[31] Amadou Gueye, FarbaBouyagui Tamboura, Adama Sy, Gaye Mohamed, Nathalie Gruber, Abdelaziz Jouait, Six new transition metal mononuclear complexes of N'-(5- bromo-2-hydroxybenzylidene)nicotinohydrazide schiff base. Synthesis, spectroscopic characterization and X-ray structure determination of the zinc(II) complex, IOSR Journal of Applied Chemistry (IOSR-JAC),April 12 (4) (2019) 24–30.

[32] Adnan Zahirović, Irnesa Osmanković, Amar Osmanović, Aleksandar Višnjevac, Amina Magoda, Selma Hadžalić, Emira Kahrović, Interaction of copper(II) complexes of bidentate benzaldehyde nicotinic acid hydrazones with BSA: spectrofluorimetric and molecular docking approach, Acta Chim. Slov. 70 (2023) 74–85.

[33] Kawther Adeeb Hussein, Naser Shaalan, Synthesis, characterization, and antibacterial activity of lanthanide metal complexes with schiff base ligand produced from reaction of 4,4-methylene diantipyrine with ethylenediamine, Indones. J. Chem. 22 (5) (2022) 1365–1375.

[34] Fatou Dioufa , Elhadj Alioune FallbFarbaBouyaguiTambouraa , Mohamed Gayeb , Nathalie Gruberc , Abdel Aziz Jouaitic, Synthesis, Spectroscopic Characterization, and Crystal Structures of Schiff Bases Derived from Nicotinic Hydrazide.

[35] Hasan Tanak, Aysen Alaman Agar, Orhan Büyükgüngör, Experimental (XRD, FT-IR and UV–Vis) and theoretical modeling studies of Schiff base (E)-N0 -, (5-nitrothiophen-2-yl)methylene)- 2-phenoxyaniline Spectrochemica Acta Part A: Molecular and Biomolecular Spectroscopy 118 (24 January) (2014) 672–682.

[36] A.A.M. Belal, I.M. El-Deen, N.Y. Farid, R. Zakaria, M.S. Refat, Synthesis, spectroscopic, coordination and biological activities of some transition metal complexes containing ONO tridentate Schiff base ligand, Spectrochim. Acta Mol. Biomol. Spectrosc. 149 (2015) 771–787.

[37] Savitha Devaswamparambil Pradeep1, Deepa Sebastian1, Anjali Krishna Gopalakrishnan1, Divya Kizhakkeppurath Manoharan1, Dhanya Thaikatt Madhusudhanan1, Puzhavoorparambil V. Mohanan, Synthesis and characterization of a novel heterocyclic schiff base and development of a fluorescent sensor for vitamin B12, J. Fluoresc. 31 (2021) 1113–1123.

[38] VALARMATHY GOVINDARAJ SUBBALAKSHMI RAMANATHAN, Synthesis, spectral characterisation, electrochemical, and fluorescence studies of biologically active novel Schiff base complexes derived from E-4-(2-hydroxy-3-methoxybenzlideneamino)-N- (pyrimidin-2-yl)benzenesulfonamide, Turk. J. Chem. 38 (2014) 521–530.

[39] Raj S. Anila, V.G. Vidya, V. Preethi, V.G. Viju Kumar, Single crystal XRD and DFT investigation of 1,5-dimethyl-4-[(2-oxo-1,2-diphenylethylidene) amino]-2-phenyl-1,2-dihydro-3H-pyrazol-3-one, Results in Chemistry 4 (2022) 10066.

[40] Iman Rajaeia , Seyed NezamoddinMirsattari, Spectroscopic characteristic (FT-IR, 1H, 13C NMR and UV-Vis) and theoretical calculations (MEP, DOS, HOMO-LUMO, PES, NBO analysis and keto–enol tautomerism) of new tetradentate N,N′-bis(4- hydroxysalicylidene)-1,4-phenylenediamine ligand as chelating agent for the synthesis of the dinuclear Co(II), Ni(II), Cu(II) and Zn(II) complexes,Journal of Molecular Structure, MOLSTR 24832.

[41] Sofian Gatfaoui, Noureddine Issaoui, Thierry Roisnel, Houda Marouani, Synthesis, experimental and computational study of a non-centrosymmetric material 3-methylbenzylammonium trioxonitrate, J. Mol. Struct. 1225 (2020) 129132.

[42] Chaima Daghar, Noureddine Issaoui, Thierry Roisnel, Dorcet Vincent, Houda Marouani, Empirical and computational studies on newly synthesis cyclohexylammonium perchlorate, J. Mol. Struct. 1230 (2021) 129820.

[43] Ferid Hammami, Noureddine Issaoui, Salah Nasr, Investigation of hydrogen bonded structure of urea-water mixtures through Infra-red spectroscopy and non-covalent interaction (NCI) theoretical approach, Computational and Theoretical Chemistry 1199 (2021) 113218.

[44] Mouna Medimagh, Cherifa Ben Mleh, Noureddine Issaoui, Aleksandr S. Kazachenko, Thierry Roisnel, Omar M. Al-Dossary, Houda Marouani, Leda G. Bousiakoug, DFT and molecular docking study of the effect of a green solvent (water and DMSO) on the structure, MEP, and FMOs of the 1-ethylpipera-zine1,4-diium bis(hydrogenoxalate), J. Mol. Liq. 369 (2023) 120851.

[45] Noureddine Mhadhbi, Noureddine Issaoui, Walid S. Hamadou, Jahoor M. Alam, Abdelmonein S. Elhadi, Mohd Adnan, Houcine Naïli, Riadh Badraoui, Physico-Chemical Properties, Pharmacokinetics, molecular docking and in-vitro pharmacological study of a cobalt (II) complex based on 2-aminopyridine, ChemistrySelect 7 (1 of 9) (2022) e202103592.

[46] Fatmah A.M. Al-Omary, Y. Sheena Mary, C. Yohannan Panicker, Ali A. El-Emam, Ibrahim A. Al-Swaidan, Abdulaziz A. Al-Saadi, C. Van Alsenoy, Spectroscopic investigations, NBO, HOMO–LUMO, NLO analysis ,and molecular docking of 5-(adamantan-1-yl)-3-anilinomethyl-2,3-dihydro1,3,4-oxadiazole-2-thione, a potential bioactive agent, J. Mol. Struct. 1096 (2015) 1–14.

[47] M.S. Meenukutty, Arsha P. Mohan, V.G. Vidya, V.G. Viju Kumar, Synthesis, characterization, DFT analysis and docking studies of a novel Schiff base using 5-bromo salicylaldehyde and β-alanine, Heliyon 8 (2022) e09600.

[48] Songül Sahin, Necmi DegeSynthesis, characterization, X-ray, HOMO-LUMO, MEP, FT-IR, NLO, Hirshfeld surface, ADMET, boiled-egg model properties and molecular docking studies with human cyclophilin D (CypD) of a Schiff base compound: (E)-1-(5-nitro-2-(piperidin-1-yl)phenyl)-N-(3-nitrophenyl) methanimine, Polyhedron 205 (2021) 115320.

[49] Sajjad Hussain Sumrra, Wardha Zafar, Sabaahatul Ain Malik, Khalid Mahmood, Syed Salman Shafqat, Saira Arif, Metal based bioactive nitrogen and oxygen donor mono and bis schiff bases: design, synthesis, spectral characterization, computational analysis and antibacterial screening, Acta Chim. Slov. (2022) 69.

[50] Sheikh Abdul Majid, Jan Mohammad Mir, Muzzaffar A. Bhat, Aabid Hussain Shalla, Abhishek Pandey, Taibi Ben Hadda, Magda H. Abdellattif, A pair of carbazate derivatives as novel Schiff base ligands: DFT and POM theory supported spectroscopic and biological evaluation, J. Biomol. Struct. Dynam. (June) (2022).

[51] A. Chitra Devi, V. Siva, S. Thangarasub, S. Athimoolamd, S. Asath Bahadur, Supramolecular architecture, thermal, Quantum chemical analysis and in vitro biological properties on sulfate salt of 4-aminoantipyrine, J. Mol. Struct. 1245 (2021) 131033.

[52] Fatmah M. Alkhatib, Hajar Mubashir Alsulami, Synthesis, characterization, DFT calculations and biological activity of new Schiff base complexes, Heliyon 9 (2023) e18988.

[53] Hossein Pasha Ebrahimi, Jabbar S. Hadi, Zuhair A. Abdulnabi, Zeinab Bolandnazar, Spectroscopic, thermal analysis and DFT computational studies of salen-type Schiff base complexes, Spectrochim. Acta Mol. Biomol. Spectrosc. 117 (2014) 485–492.

[54] Subhash Mamta, Ashu Chaudhary Pinki, In vitro cytotoxicity and antimicrobial evaluation of novel 24–28 membered Schiff base octaazamacrocyclic complexes of manganese(II): synthesis, characterization, DFT and molecular docking studies, J. Mol. Struct. 1275 (2023) 134667.

[55] C. Valgas, S.M. De Souza, E.F.A. Smánia, et al., Screening methods to determine antibacterial activity of natural products Braz, J. Microbiol. 38 (2007) 369–380.

[56] S. Magaldi, S. Mata-Essayag, C. Hartung de Capriles, et al., Well diffusion for antifungal susceptibility testing, Int. J. Infect. Dis. 8 (2004) 39–45.

[57] T. Mosmann, Rapid colorimetric assay for cellular growth and survival: application to proliferation and cytotoxicity assays, J. Immunol. Methods 65 (1983) 55–63.

[58] Subhash, A. Chaudhary, Mamta, Jyoti, Synthesis, structural characterization, thermal analysis, DFT, biocidal evaluation and molecular docking studies of amide-based Co(II) complexes, Chem. Paper Slovak Acad. Sci. 77 (2023) 5059–5078.

[59] M.M. Joseph, S.R. Aravind, S. Varghese, S. Mini, T.T. Sreelekha, Evaluation of antioxidant, antitumor and immunomodulatory properties of polysaccharide isolated from fruit rind of Punicagranatum, Mol. Med. Rep. 5 (2) (1983) 489–496.

[60] Shweta Agarwal and Ranjana Mehrotra, An overview of molecular docking, JSM Chem 4(2):1024..

[61] Yang Liu, Maximilian Grimm, Wen-tao Dai, Mu-chun Hou, Zhi-Xiong Xiao, Yang Cao, CB-Dock: a web server for cavity detection-guided protein–ligand blind docking, Acta Pharmacol. Sin. 41 (2020) pages138–144.

[62] Tomris Coban, Cameron Robertson, Sianne Schwikkard, Richard Singer, Adam LeGresley, Synthesis and evaluation of bis(imino)anthracene derivatives as G-quadruplex ligands, RSC Med. Chem. 12 (2021) 751–757.

[63] Yang Liu, Xiaocong Yang, Jianhong Gan, Shuang Chen, Zhi-Xiong Xiao, Yang Cao, CB-Dock2: improved protein–ligand blind docking by integrating cavity detection, docking and homologous template fitting, Nucleic Acids Res. 50 (2022).

[64] Nicolás Flores-Castañón, Shrabana Sarkar, Aparna Banerjee, Structural, functional, and molecular docking analyses of microbial cutinase enzymes against polyurethane monomers, Journal of Hazardous Materials Letters 3 (2022) 100063.

[65] Muhammed Amanat, Muhammad Tawhid , A.F.M Shahid-Ud-Daula, Anthelmintic activity of Zingiber roseum rhizomes against Pheretima posthuma: in vitro and in silico approach, International Journal of Scientific Research in Chemistry (IJSRCH) © 2022 IJSRCH| Volume 7 | Issue 1 | ISSN : 2456-8457.

[66] Kavitha Bharatham, Ki Hun Park NagakumarBharatham, Keun Woo Lee, Binding mode analyses and pharmacophore model development for sulfonamide chalcone derivatives, a new class of a-glucosidase inhibitors, J. Mol. Graph. Model. 26 (2008) 1202–1212.

[67] Manish Kumar Subhash, Anita Phor, Monika Gupta, Ashu Chaudhary, Design, synthesis, characterization, in vitro cytotoxic, antimicrobial, antioxidant studies, DFT, thermal and molecular docking evaluation of biocompatible Co(II) complexes of N4O4-macrocyclic ligands, Comput. Biol. Chem. 110 (2024) 10803.

[68] Yang Liu, Xiaocong Yang, Jianhong Gan, Shuang Chen, Zhi-Xiong Xiao, Yang Cao, CB-Dock2: improved protein–ligand blind docking by integrating cavity detection, docking and homologous template fitting, Nucleic Acids Res. 50 (2022).

[69] ShinuChacko ReetuparnaAcharya1, Pritha Bose, Antonio Lapenna, Shakti Prasad Pattanayak, Structure based multitargeted molecular docking analysis of selected furanocoumarins against breast cancer, Scientific Reports nature research 9 (2019) 15743.

[70] Anitha Kumari Vinjavarapu, Shaheen Begum, Bharathi Koganti, Synthesis, evaluation, and in silico studies of 2-mercapto-5-substituted styryl-1,3,4-oxadiazoles as potential cytotoxic agents, the Thai, J. Pharmaceut. Sci. 44 (1) (2020).

[71] Hany A.M. El-Sherief, Bahaa G.M. Youssif, Syed Nasir Abbas Bukhari, Ahmed H. Abdelazeem, Mohamed Abdel-Aziz, Hamdy M. Abdel-Rahman, Synthesis, anticancer activity and molecular modeling studies of 1,2,4-triazole derivatives as EGFR inhibitors, Eur. J. Med. Chem. 156 (2018) 774e789.

[72] M.H. Hofmann, R. Mani, H. Engelhardt, M.A. Impagnatiello, S. Carotta, M. Kerenyi, S. Lorenzo-Herrero, J. Böttcher, D. Scharn, H. Arnhof, A. Zoephel, R. Schnitzer, T. Gerstberger, M.P. Sanderson, G. Rajgolikar, S. Goswami, S. Vasu, P. Ettmayer, S. Gonzalez, M. Pearson, D.B. McConnell, N. Kraut, N. Muthusamy, J. Moll, Selective and potent CDK8/19 inhibitors enhance NK cell activity and promote tumor surveillance, Mol. Cancer Ther. 19 (4) (2020) 1018–1030.

[73] Roni H.G. Wright, Miguel Beato, Role of the NUDT enzymes in breast cancer, Int. J. Mol. Sci. 22 (2021) 2267.